Vibration insensitive extended range interference microscopy

Joshua T. Wiersma[1,2,*] and James C. Wyant[1,2]

[1]4D Technology Corporation, 3280 E. Hemisphere Loop, Ste. 146, Tucson, Arizona 85706, USA

[2]College of Optical Sciences, The University of Arizona, 1630 E. University Blvd., Tucson, Arizona 85721, USA

*Corresponding author: jtwiersma@gmail.com

Received 11 March 2013; revised 29 May 2013; accepted 23 July 2013;
posted 24 July 2013 (Doc. ID 186802); published 14 August 2013

Using a simultaneous phase sensor, the proposed instrument performs highly repeatable measurements over an extended range in the presence of vibration common to a laboratory setting. Measurement of a 4.5 μm step standard in the presence of vibration amplitudes of 40 nm produces a repeatability of 1.5 nm RMS with vertical scanning data acquired at 400 nm intervals. The outlined method demonstrates the potential to tolerate larger vibration amplitudes up to or beyond a quarter wavelength and to increase the data acquisition step size to that approaching the depth of field of standard microscope imaging systems. © 2013 Optical Society of America

OCIS codes: (120.2830) Height measurements; (120.3180) Interferometry; (120.3940) Metrology; (120.4290) Nondestructive testing; (120.5050) Phase measurement; (180.3170) Interference microscopy.
http://dx.doi.org/10.1364/AO.52.005957

1. Introduction

Calculating the relative phase of the wavefront emanating from a test surface using phase shifting interferometry (PSI) provides the most repeatable measurements in interference microscopy [1]. Unfortunately, single-wavelength techniques suffer from ambiguities due to the periodic nature of the interference patterns when the test surface possesses discontinuities exceeding a quarter wavelength. Many algorithms employ coarser vertical scanning interferometry (VSI) profiles by estimating the localization of high-contrast fringes in space to unwrap the phase information and overcome the aforementioned ambiguity. However, while these phase unwrapping algorithms extend the vertical range, they use data acquired temporally, meaning the instrument obtains a minimum of three phase-shifted interferograms sequentially in time [2–9].

1559-128X/13/245957-05$15.00/0
© 2013 Optical Society of America

Temporal methods result in a measurement technique vulnerable to errors induced by vibration changing the relative orientation of the instrument and test surface during data acquisition. In most implementations, a change in the optical path difference between the test surface and the instrument induces the desired phase shift. The most common algorithms use 90° phase shifts, which require eighth wave movements when accounting for the double pass of the wavefront when measuring in reflection. [10]. Accordingly, even small vibrations can significantly change the effective phase shift and introduce errors into the measurement [11].

The proposed method captures four phase-shifted interference patterns simultaneously by using a pixelated mask camera [12,13]. The pixelated mask consists of four orientations of microwire grid polarizers, which induce a geometric phase shift when presented with left and right circularly polarized light from the test and reference beams. A single camera frame contains all the information necessary to calculate the phase, thus reducing the error introduced by vibration.

Furthermore, capturing virtually instantaneous phase values along the vertical scan allows for a more accurate characterization of the distance between the test and reference surface at each camera frame acquisition in the presence of vibration. Modern vertical scanning mechanisms provide an extremely linear motion, allowing an average step size to accurately characterize the distance traveled between camera frames when using a fixed frame rate. However, vibration changes the distance between the test and reference surface independent of the scanning mechanism. Subtraction of phase values at successive points in the vertical scan allows construction of an accurate profile of the relative position of the test and reference surfaces during the scan even in the presence of vibration. The primary unwrapping of the phase to the VSI profile benefits from this additional information, which characterizes and removes the errors introduced by vibration. The method presented here leverages virtually instantaneous phase values to produce measurements with the repeatability of single-wavelength PSI over an extended range in the presence of mild vibration [14].

2. Instrument Overview

The instrument consists of a polarization-based interference microscope in a Michelson configuration with a pixelated mask camera. An approximate layout found in Fig. 1 shows a roughly 2 mm square light-emitting diode (LED) source with a center wavelength of 460 nm and a full width at half-maximum spectrum of 30 nm. Two lenses reimage the source to a plane coincident with the aperture stop, which, along with any vignetting by the lenses, controls the effective numerical aperture and subsequently the spatial coherence as well as the resolution of the imaging system. The following lens pseudocollimates the source, while the field stop controls the extent of the test surface illumination. The next lens images the LED and aperture stop into the entrance pupil of the 2× microscope objective, which provides Köhler illumination to the test and reference surfaces. A linear polarizer sets the polarization of the unpolarized source (surrendering 50% of the light) and controls the beam balance between the interferometer arms in conjunction with a polarizing beam splitter (PBS) cube. A non-PBS (NPBS) cube folds the imaging arm consisting of a tube lens and camera into the optical path (again surrendering 50% of the light with each pass). A quarter-wave plate (QWP) circularizes the orthogonal polarizations from the test and reference arms before the light impinges upon the camera. A pixelated mask consisting of patterned microwire grid polarizers aligned with each pixel, as shown in Fig. 2, sits just in front of the camera and induces a geometric phase shift (again surrendering 50% of the light) [15,16]. The camera consists of a square sensor with 1200 pixels on a side resulting in a 4.4 mm field of view. A closed loop piezoelectric transducer (PZT) pistons the Michelson objective, consisting of the elements pictured below the PZT *sans* the test object (Fig. 1), over a 30 μm range.

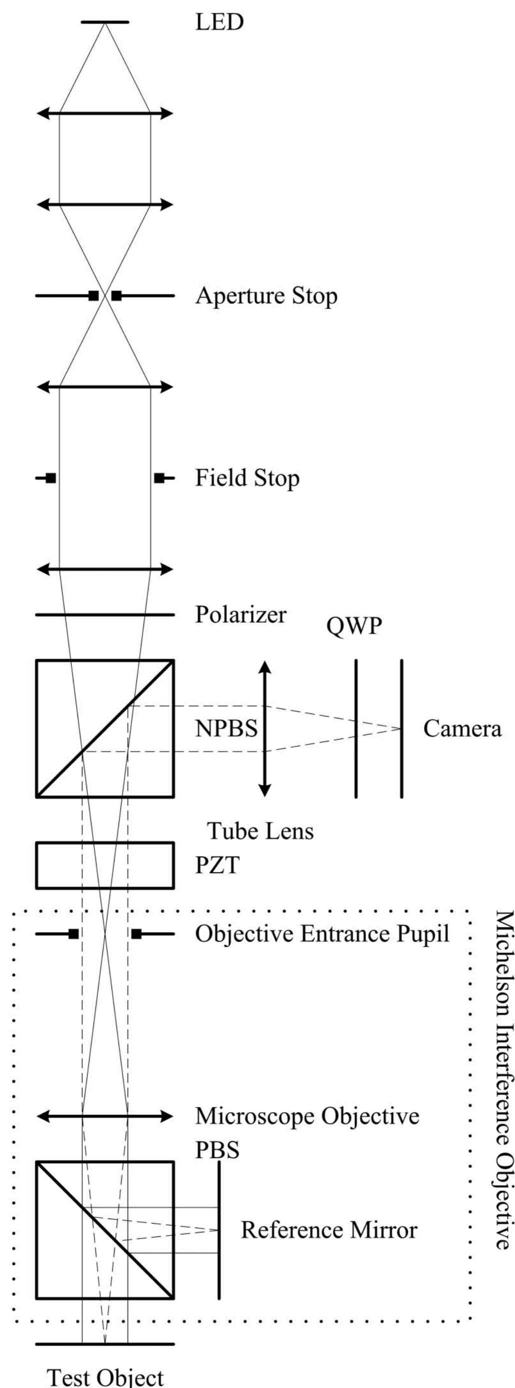

Fig. 1. Overview of a polarization-based interference microscope in a Michelson configuration equipped with a pixelated mask camera.

3. Data Acquisition and Processing

The user places the test surface near the middle of the scan range and nulls the tilt fringes. For the measurements disseminated here, the instrument vertically scans the test object with a ramping motion while capturing a camera frame every 400 nm.

0°	90°	0°	90°	0°	90°
270°	180°	270°	180°	270°	180°
0°	90°	0°	90°	0°	90°
270°	180°	270°	180°	270°	180°
0°	90°	0°	90°	0°	90°
270°	180°	270°	180°	270°	180°

Fig. 2. Sample of the pixelated mask phase shift pattern.

The system does not use any active or passive vibration isolation methods.

After scan completion, an algorithm uses successive phase values to calculate the relative position of the test and reference surface throughout the scan, allowing a more accurate unwrapping of the phase to the VSI profile [17]. The algorithm subtracts sequential phase values from the scan where the fringe visibility exceeds 20% and unwraps the phase difference to the average acquisition step size of 400 nm expected in the absence of vibration. If the vibration magnitude exceeds a quarter wavelength, an unwrapping error resulting in the wrong step size occurs. The coherence of the source allows greater than 20% fringe visibility over approximately 5 μm along the vertical axis. Thus the source's coherence length limits the instrument's ability to measure samples with global vertical discontinuities greater than 10 μm because of an inability to construct a continuous scan profile.

Figure 3 depicts the vibration profile of the laboratory setting during acquisition of the presented measurements created using the aforementioned phase subtraction methodology. The vibration profile shows the departure of each data acquisition step from the expected step size. The environment presented here

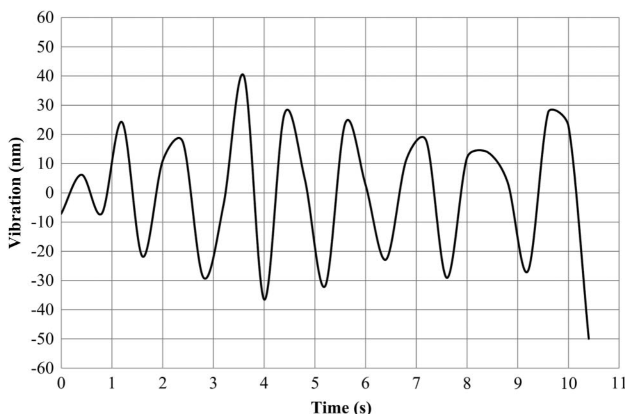

Fig. 3. Vibration profile during data acquisition.

demonstrates a vibration magnitude of roughly 40 nm while the current algorithm can handle a maximum magnitude of 115 nm based on the center wavelength of the source. However, adding a distance measuring interferometer, which does not suffer from phase unwrapping ambiguities, to the system would allow the instrument to measure vibration profiles beyond 115 nm in amplitude and discontinuities larger than 10 μm [18].

Having the scan profile account for the influence of vibration allows a more accurate unwrapping of the phase to the VSI profile. A least-squares Gaussian fit of the modulation data as a function of the scan profile generates a coarse surface profile allowing pixel-independent unwrapping of the phase as shown in Fig. 4. The algorithm selects the phase value with the highest fringe contrast, adds the scan position, and unwraps the sum to the VSI profile using conventional methods.

The program uses traditional four-bucket recipes to calculate the modulation and phase values for each camera frame at each step [19]. An additional processing step removes tilt induced by dispersion from the VSI data before unwrapping. Manufacturing errors in the polarizing cube beam splitter in the Michelson objective coupled with dispersion effects from the extended source account for the extraneous tilt. The use of a Mirau objective may reduce the optical path asymmetry, since fabricators can often hold plate beam splitters to tighter tolerances [20]. The errant tilt shifts the peak of the coherence envelope without affecting the phase—at least for samples with small slopes [21].

Generation and subtraction of an instrument reference by measuring a well-nulled flat surface allows removal of the tilt from the VSI measurement. However, in the current design, the measured instrument reference changes slightly over time due to thermal effects altering the pointing of the light through the beam splitter as well as the shape of the beam splitter itself. A data acquisition step size of 400 nm results in few unwrapping errors, and the step size may increase in the future if mitigation of the thermal effects improves the stability of the instrument.

4. Results

The measurement of an approximately 4.5 μm step standard demonstrates the ability of the instrument

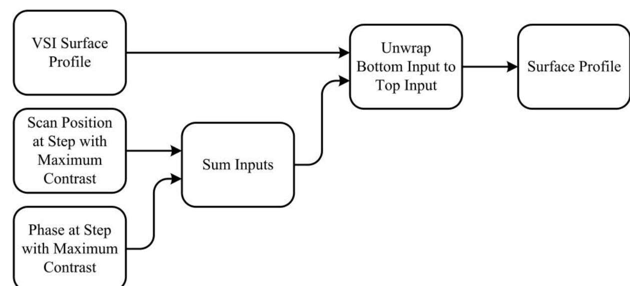

Fig. 4. Unwrapping algorithm using a coarse VSI profile to remove ambiguities in the phase.

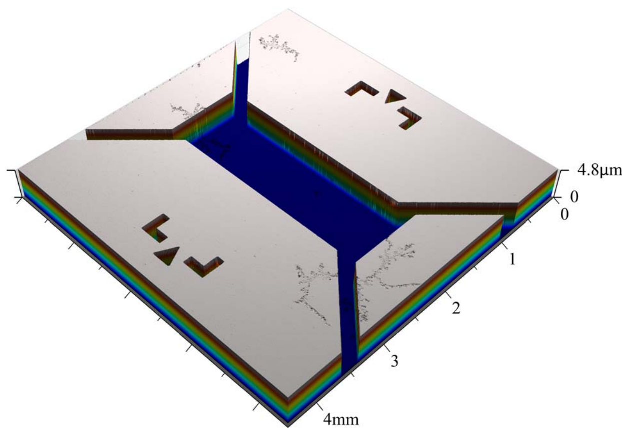

Fig. 5. Measurement of a 4.5 μm step.

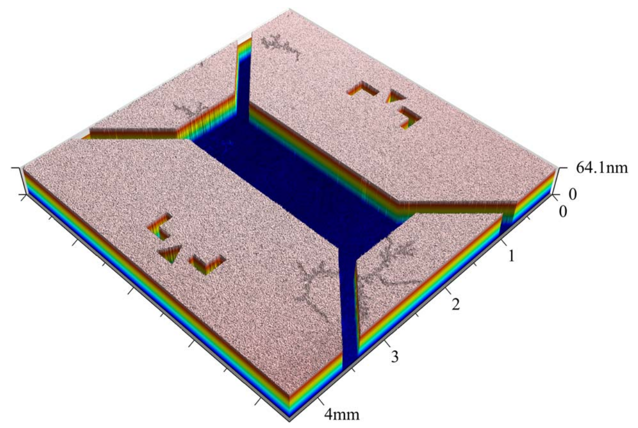

Fig. 7. Repeatability of the measurement of a 4.5 μm step using the average data acquisition step size.

to make repeatable measurements over an extended range in the presence of vibration. The unwrapped phase of the step measurement in Fig. 5 shows some damage to the quartz standard's 90 nm thick chromium coating in the form of curling fissures.

The ability to scale the measurement of the absolute size of the step to a known standard imparts more importance in the repeatability of the measurements. All commercial interferometers use a scaling factor set by measuring a known reference height to account for the effective wavelength of the extended source as well as the numerical aperture factor of the microscope objective [22]. The point-by-point subtraction of two measurements of the step reveals a repeatability of 1.5 nm RMS as shown in Fig. 6. The pixelated mask enables the measurement of and compensation for the vibration present during data acquisition, which results in highly repeatable measurements.

For comparison, if the algorithm uses the average step size rather than the actual step size, the repeatability dramatically decreases as seen in Fig. 7. In this case the measured step size varied roughly 60 nm between the two measurements, whereas the noise in the phase essentially limits the repeatability when using the calculated step size [23]. In this example the vibration largely results in a pistoning movement. Implementation of the algorithm across the field could allow for correction of a relative tilt between the test sample and the instrument.

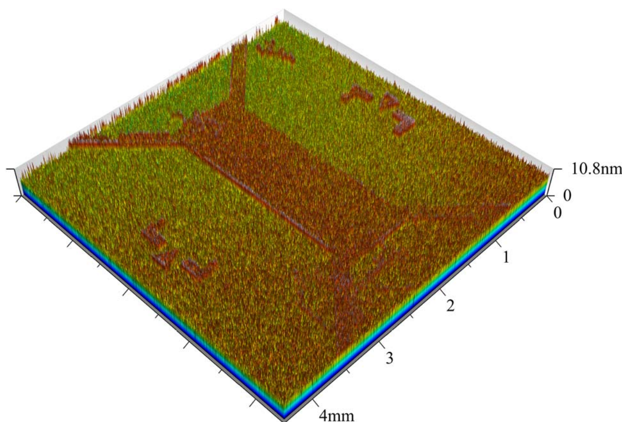

Fig. 6. 1.5 nm RMS repeatability of the measurement of a 4.5 μm step using measured data acquisition step sizes.

5. Future Work

The presented results demonstrate great promise for a highly repeatable interference microscopy technique with extended range and vibration insensitivity. However, the capabilities of the instrument require further characterization by measuring various samples in different settings.

One such instance may include characterizing the surface roughness of large telescope mirrors during the various stages of polishing. The vibration insensitivity of the instrument allows placement directly on the telescope surface allowing the capture of low-noise measurements as the surface roughness decreases. Measurement of optically rough surfaces often occurs using a pure VSI mode, and this instrument offers advantages here as well by capturing the modulation values virtually instantaneously and averaging out the vibration using a Gaussian fitting routine.

A future redesign of the instrument could easily incorporate an extended scan range beyond the 30 μm used for the proof of concept. In addition, the instrument shows capacity for an increased data acquisition step size beyond the 400 nm demonstrated that would push the limits of the depth of field of standard microscope imaging systems. The instrument already enables a step size five times larger than most commercial instruments, which results in the reduction of acquisition times and further enhances the dynamic ability of the instrument.

Furthermore, the results demonstrate a reduced sensitivity to a diffraction phenomena commonly found in VSI measurements known as "bat-wings," which induces ringing at certain discontinuities on the test sample [24,25]. However, future work with a variety of sample heights must confirm the reduced sensitivity to this undesirable diffraction effect.

6. Conclusion

The proposed instrument leverages the advantages of a simultaneous phase sensor to produce repeatable measurements over an extended range in the presence of mild vibration. The instrument captures phase values in the presence of vibration using a pixelated mask camera to obtain four phase-shifted interferograms simultaneously. A vertical scan of the test surface coupled with a low-coherence source allows the construction of a coarse surface profile using modulation values calculated from the phase-shifted interferograms. A Gaussian fit of the modulation values over the length of the scan yields a rough surface profile while averaging out the influence of vibration. The coarse surface profile enables the extended range of the instrument through an unwrapping process, which removes the periodic ambiguities in the phase data. Furthermore, the subtraction of successive phase values and subsequent construction of a scan profile allows the characterization and removal of mild vibration from the measurement.

A prototype of the described instrument uses a 400 nm data acquisition step size to produce measurements of a 4.5 μm step with a repeatability of 1.5 nm RMS in the presence of vibration amplitudes of 40 nm. The instrument possesses the capacity to increase both the vibration amplitude tolerance as well as the data acquisition step size.

References

1. J. Schmit, K. Creath, and J. C. Wyant, "Surface profilers, multiple wavelength, and white light interferometry," in *Optical Shop Testing*, D. Malacara, ed. (Wiley, 2007), pp. 667–755.
2. D. K. Cohen, P. J. Caber, and C. P. Brophy, "Rough surface profiler and method," U.S. patent 5,133,601 (28 July 1992).
3. C. Ai and P. J. Caber, "Combination of white-light scanning and phase-shifting interferometry for surface profile measurements," U.S. patent 5,471,303 (28 November 1995).
4. K. G. Larkin, "Efficient nonlinear algorithm for envelope detection in white light interferometry," J. Opt. Soc. Am. A **13**, 832–843 (1996).
5. P. Sandoz, R. Devillers, and A. Plata, "Unambiguous profilometry by fringe-order identification in white-light phase-shifting interferometry," J. Mod. Opt. **44**, 519–534 (1997).
6. R. Windecker, M. Fleischer, and H. J. Tiziani, "White-light interferometry with an extended zoom range," J. Mod. Opt. **46**, 1123–1135 (1999).
7. A. Harasaki, J. Schmit, and J. C. Wyant, "Improved vertical-scanning interferometry," Appl. Opt. **39**, 2107–2115 (2000).
8. P. de Groot and J. W. Kramer, "Height scanning interferometry method and apparatus including phase gap analysis," U.S. patent 6,775,006 (10 August 2004).
9. D. Chen, "High-definition vertical-scan interferometry," U.S. patent 7,605,925 (20 October 2009).
10. H. Schreiber and J. H. Bruning, "Phase shifting interferometry," in *Optical Shop Testing*, D. Malacara, ed. (Wiley, 2007), pp. 547–666.
11. P. J. de Groot and L. L. Deck, "Numerical simulations of vibration in phase-shifting interferometry," Appl. Opt. **35**, 2172–2178 (1996).
12. C. Dunsby, Y. Gu, and P. M. W. French, "Single-shot phase-stepped wide-field coherence-gated imaging," Opt. Express **11**, 105–115 (2003).
13. J. Millerd, N. Brock, J. Hayes, M. North-Morris, M. Novak, and J. Wyant, "Pixelated phase-mask dynamic interferometer," Proc. SPIE **5531**, 304–314 (2004).
14. J. T. Wiersma, "Pixelated mask polarization based spatial carrier interference microscopy," Ph.D. thesis (University of Arizona, Tucson, 2012).
15. P. Hariharan and M. Roy, "White-light phase-stepping interferometry for surface profiling," J. Mod. Opt. **41**, 2197–2201 (1994).
16. M. Roy, P. Svahn, L. Cherel, and C. J. R. Sheppard, "Geometric phase-shifting for low-coherence interference microscopy," Opt. Lasers Eng. **37**, 631–641 (2002).
17. J. Schmit and A. Olszak, "High-precision shape measurement by white-light interferometry with real-time scanner error correction," Appl. Opt. **41**, 5943–5950 (2002).
18. A. Olszak and J. Schmit, "High-stability white-light interferometry with reference signal for real-time correction of scanning errors," Opt. Eng. **42**, 54–59 (2003).
19. E. P. Goodwin and J. C. Wyant, *Field Guide to Interferometric Optical Testing* (SPIE, 2006).
20. J. Schmit and P. Hariharan, "Improved polarization Mirau interference microscope," Opt. Eng. **46**, 077007 (2007).
21. A. Pförtner and J. Schwider, "Dispersion error in white-light Linnik interferometers and its implications for evaluation procedures," Appl. Opt. **40**, 6223–6228 (2001).
22. K. Creath, "Calibration of numerical aperture effects in interferometric microscope objectives," Appl. Opt. **28**, 3333–3338 (1989).
23. B. Kimbrough, N. Brock, and J. Millerd, "Dynamic surface roughness profiler," Proc. SPIE **8126**, 81260H (2011).
24. A. Harasaki and J. C. Wyant, "Fringe modulation skewing effect in white-light vertical scanning interferometry," Appl. Opt. **39**, 2101–2106 (2000).
25. M. Roy, J. Schmit, and P. Hariharan, "White-light interference microscopy: minimization of spurious diffraction effects by geometric phase-shifting," Opt. Express **17**, 4495–4499 (2009).